Original

von Storch, H.; Feser, F.; Geyer, B.; Klehmet, K.; Li, D.; Rockel, B.; Schubert-Frisius, M.; Tim, N.; Zorita, E.:
Regional reanalysis without local data: Exploiting the downscaling paradigm.
In: Journal of Geophysical Research : Atmospheres. Vol. 122 (2017) 16, 8631 - 8649.
First published online by AGU: 11.08.2017

https://dx.doi.org/10.1002/2016JD026332

AGU PUBLICATIONS

JGR

Journal of Geophysical Research: Atmospheres

RESEARCH ARTICLE
10.1002/2016JD026332

Key Point:
- Consistent regional reanalyses can be generated through dynamical downcsaling in data sparse regions. Global downscaling results in a skill comparable to regional downscaling

Correspondence to:
H. von Storch,
hvonstorch@web.de

Citation:
von Storch, H., F. Feser, B. Geyer, K. Klehmet, D. Li, B. Rockel, M. Schubert-Frisius, N. Tim, and E. Zorita (2017), Regional reanalysis without local data: Exploiting the downscaling paradigm, *J. Geophys. Res. Atmos.*, *122*, 8631–8649, doi:10.1002/2016JD026332.

Received 4 DEC 2016
Accepted 25 JUL 2017
Accepted article online 11 AUG 2017
Published online 29 AUG 2017

Regional reanalysis without local data: Exploiting the downscaling paradigm

Hans von Storch[1,2], Frauke Feser[1,2], Beate Geyer[1], Katharina Klehmet[1], Delei Li[3], Burkhardt Rockel[1], Martina Schubert-Frisius[1,2], Nele Tim[4], and Eduardo Zorita[1]

[1]Institute of Coastal Research, Helmholtz Zentrum Geesthacht, Geesthacht, Germany, [2]CliSAP, University of Hamburg, Hamburg, Germany, [3]Institute of Oceanology, Chinese Academy of Sciences, Qingdao, China, [4]Institute for Geology, University of Hamburg, Hamburg, Germany

Abstract This paper demonstrates two important aspects of regional dynamical downscaling of multidecadal atmospheric reanalysis. First, that in this way skillful regional descriptions of multidecadal climate variability may be constructed in regions with little or no local data. Second, that the concept of large-scale constraining allows global downscaling, so that global reanalyses may be completed by additions of consistent detail in all regions of the world. Global reanalyses suffer from inhomogeneities. However, their *large-scale componenst* are mostly homogeneous; Therefore, the concept of downscaling may be applied to homogeneously complement the large-scale state of the reanalyses *with regional detail*—wherever the condition of homogeneity of the description of large scales is fulfilled. Technically, this can be done by dynamical downscaling using a regional or global climate model, which's large scales are constrained by spectral nudging. This approach has been developed and tested for the region of Europe, and a skillful representation of regional weather risks—in particular marine risks—was identified. We have run this system in regions with reduced or absent local data coverage, such as Central Siberia, the Bohai and Yellow Sea, Southwestern Africa, and the South Atlantic. Also, a global simulation was computed, which adds regional features to prescribed global dynamics. Our cases demonstrate that spatially detailed reconstructions of the climate state and its change in the recent three to six decades add useful supplementary information to existing observational data for midlatitude and subtropical regions of the world.

Plain Language Summary This paper demonstrates two important aspects of regional dynamical downscaling of multidecadal atmospheric reanalysis. First, in this way, skillful regional descriptions of multidecadal climate variability may be constructed in regions with little or no local data. Secondly, the concept of large-scale constraining allows global dynamical downscaling so that global reanalyses may be completed by additions of consistent detail in all regions of the world.

1. Introduction

When planning for maintenance of offshore structures, when designing ships to withstand environmental stresses, when assessing the risk of very high storm surges [*Weisse et al*., 2009, 2014, 2015] or the potential of wind energy [*Geyer et al*., 2015; *Li et al*., 2016a], of the variability of regional upwelling [*Tim et al*., 2015], implications on permafrost thermal state, ecology, and biochemical cycles through snow cover and depth [*Klehmet et al*., 2013], realistic descriptions of the regionally detailed weather stream for a sufficiently long time are needed. Such descriptions or analyses cannot be constructed directly from observations simply because of scarcity of observational data. "Long" time series are needed to describe the range of variations, interdecadal variability, and change. In most cases several decades of data will be needed for such assessments. Another condition for such analyses is that they are homogeneous; i.e., changes across time and space are related to variability in weather patterns and frequencies and not due to changing instrumentation, time of recording, built, and natural environment etc. [e.g., *Karl et al*., 1993]. Using a "frozen" reanalysis model for guiding the analysis is insufficient for guaranteeing homogeneity when the database is changing in time and space. The latter problem is likely unavoidable.

There are now a series of *global reanalyses* covering several decades or longer, which are generated from an objective combination of numerical models and conventional observations and/or satellite-data based on a specific unchanging data assimilation scheme. According to the incremental advancement of reanalysis techniques, three generations of reanalysis data sets are classified, from the first-generation

reanalyses with initial efforts such as National Centers for Environmental Prediction 1 (NCEP1) [*Kalnay et al*., 1996] and NCEP-Department of Energy [*Kanamitsu et al*., 2002], to the second generation like ERA-40 [*Uppala et al*., 2005] and Japanese 25 year Reanalysis (JRA-25) [*Onogi et al*., 2007] assimilated with available satellite radiances, to the third generation such as ERA-Interim [*Dee et al*., 2011] and JRA-55 [*Kobayashi et al*., 2015] with adoption of sophisticated assimilation approaches (https://climatedataguide.ucar.edu/climate-data/atmospheric-reanalysis-overview-comparison-tables#Table).

Obviously, the introduction of satellite data into the analyses at the end of the 1970s lead to improvements of the data coverage and thus of the analyses—but it also went along with temporal inhomogeneities [*Kistler et al*., 2001]. This is a significant issue, in particular in the southern hemisphere [*Kalnay et al*., 1996]. Because of this, many attempts of reanalyzing set as starting time 1979 or even later. However, these analyses suffer from a limited spatial resolution, mostly with grid distances of 55–210 km, leading to poor ability to resolve regional atmospheric features. This is especially the case for areas with complex topography, such as the coasts of the Baltic Sea, which are in most cases only rudimentarily resolved.

These reanalysis data sets have been widely used for climate research and services including comparing current with past climate conditions, investigating the climate variability and change as well as preparing for climate projections [e.g., *Pryor et al*., 2009; *Larsén and Mann*, 2009; *Donat et al*., 2014].

Some more recent attempts have tried to construct reanalyses using observations from about 1900 onward (20CR [*Compo et al*., 2011] and ERA-20C [*Poli et al*., 2016]). Such efforts are to be applauded, but they do cause massively inhomogeneities for long-term analyses, mostly due to increasing station density over time, as was demonstrated for the case of storm indicators [*Krueger et al*., 2013, 2014].

In view of this problem we have developed a different setup, namely, to process the small-scale part of global reanalysis with dynamical models. We believe that the *large-scale part* of the reanalyses is relatively homogeneous: for most of the northern hemisphere since 1960 or so (later we will document an exception with an inhomogeneity in the large scales over Siberia), and in the southern hemisphere since about 1980 [*Kistler et al*., 2001]. The processing with dynamical models is done by constraining the model to stay close to the reanalysis at these "accepted" scales. A commonly used method to this end is *spectral nudging* [*Waldron et al*., 1996; *von Storch et al*., 2000] which has been shown to constrain the simulated trajectory to follow closely the large-scale component of the driving reanalyses. Related procedures were earlier suggested by *Kida et al*. [1991] and *Sasaki et al*. [1995].

This procedure that generated additional realistic details has been demonstrated earlier [e. g. *Chan et al*., 2014; *Di Luca et al*., 2012, 2015; *Feser and von Storch*, 2008a; *Feser et al*., 2011; *Parker et al*., 2015; *Prein et al*., 2013; *Winterfeldt and Weisse*, 2009; *Zahn et al*., 2008]. Thus, we are not trying to demonstrate the added value generated by dynamical downscaling, and the mechanism behind it, but we want to show that this methodology is permitting to generate realistic regional detail in data-sparse regions—and that the effort can be done globally, if sufficient computer resources are available.

Also, other concepts, in particular grid-point nudging, are in use [*Lo et al*., 2008]. In this case, all dynamical information of the driving reanalysis is used, and the expected added value concerns processes like precipitation and scales beyond the resolution of the driving "mother" model. *Liu et al*. [2012] tested simulations with grid-point nudging and with spectral nudging and found the latter superior. This was to be expected, because grid-point nudging implicitly assumes that the driving reanalysis provides robust and homogeneous information at the smallest resolved scales, which is certainly not true, given the truncation of the nonlinear interactions across scales [e.g., *von Storch*, 1978].

The downscaling concept, as put into effect by spectral nudging, has by now been widely accepted in the scientific community [e.g., *Miguez-Macho et al*., 2004; *Sotillo et al*., 2005; *Feser and von Storch*, 2008a; *Rockel et al*., 2008a; *Heikkilä et al*., 2011; *Winterfeldt et al*., 2011; *Feser and Barcikowska*, 2012; *Berg et al*., 2013; *Wang and Kotamarthi*, 2013; *Choi and Lee*, 2016]. Initially, there was some opposition, because the introduction of the correction terms would violate conservation laws of mass and momentum. Obviously, reanalyses are not constructed to strictly conserve mass and momentum, and the driving global reanalyses violate these principles. Likewise, the conservation laws are not fulfilled for the atmosphere when in contact with the ocean and other components of the climate system.

Spectral nudging has been shown to be efficient in suppressing noteworthy intraensemble variability on large scales (which is substantial for model areas of 1000 and more kilometer, when the individual simulations in the ensemble are only constrained by lower and lateral boundary conditions [*Weisse et al*., 2000, *Weisse and Feser*, 2003]). On the other hand, an added value is generated on regional and possibly local scales, where weather variability is dynamically constrained by the enforced large-scale state [*Feser et al*., 2011; *Miguez-Macho et al*., 2004].

Added value typically refers to a description by a regional model which is more detailed and physically consistent than its forcing data sets (reanalysis data or global climate model (GCMs)) [*Rummukainen*, 2015]. There are different ways to determine added value, and a failure to determine such added value with one method does not exclude the possibility that added value may show up in different assessments.

One way to identify the added value is to determine improvements of some quantitative measures of skill of the downscaled product (in most cases by regional climate models (RCMs)) relative to their forcing data sets, with observations as reference [e.g., *Lucas-Picher et al*., 2012; *Ban et al*., 2014; *Chan et al*., 2014]. Added values have been identified in variables such as precipitation, near-surface temperature, surface wind, and extremes mainly in regions with complex orography, e.g., mountainous and coastal areas [*Feldmann et al*., 2008; *Feser et al*., 2011; *Winterfeldt et al*., 2011; *Dosio et al*., 2015; *Torma et al*., 2015; *Li et al*., 2016b]. This approach may be pursued with local observations, which, however, do not allow a scale separation. Therefore, it would be useful if gridded data would be available with a spatial resolution corresponding to the downscaled product. Such homogeneous data sets do rarely exist, and if so, then only for a rather limited period. *Feser et al*. [2011] employed operational high-resolution weather forecasts which were available homogeneously for a few years. A regional reanalysis for Europe was compiled by *Dahlgren et al*. [2016] with the regional model HIgh-Resolution Limited-Area Model on a grid mesh width of 22 km.

Another approach for identifying added value is to look for mesoscale dynamical phenomena, for instance, related to orography or thermal discontinuities (e.g., at coasts and ice margins) such as mesoscale cyclones, local wind systems, or urban environments [*Feser and von Storch*, 2008b; *Zahn et al*., 2008; *Cavicchia and von Storch*, 2011; *Hamdi et al*., 2013; *Li*, 2017]. This kind of added value is generally determined by an empirical or theoretical assessment. It can also be employed when observations are unavailable as in projections of future climate conditions [e.g., *Mahoney et al*., 2012; *Hamdi et al*., 2013].

The skill of generating added value was demonstrated by *Feser et al*. [2011] in extensive studies dealing with the European region. In this region, many different data sets for assessing the skill of the downscaling effort are available and have been used to determine surface wind conditions, in particular. Systematic problems in using different data sources did not emerge. In this case not only an atmospheric reanalysis was done, but these data were also used to reanalyze maritime conditions, in particular waves [cf. *Weisse et al*., 2009, 2014, 2015]. The data for the European region have been made public [*Geyer*, 2013]; the original grid resolution was about 50 km; the present grid resolution is in many cases about 12 km [e.g., *Kotlarski et al*., 2014], but first experiments with convection-permitting resolution are presently done and evaluated.

Most spectrally nudged simulations have been done for midlatitudes and for the subtropics of both hemispheres. So far, only a few studies have considered the tropics [*Ramzan et al*., 2017]. Some attention has been paid to the climatology of typhoons [*Choi and Lee*, 2016; *Feser and von Storch*, 2008b; *Feser and Barcikowska*, 2012; *Barcikowska et al*., 2017].

A challenging question is the identification of the mechanisms which lead to the generation of added value. In principle, a series of different factors may be acting—one being a better description of the surface physiographic details, such as coastlines, mountain ranges, or sea surface/sea ice distributions, another a better description of the hydrodynamics and thermodynamics by a broader spectral range for describing the dynamic interactions, a more realistic treatment of subgrid-scale processes. Disentangling the different mechanisms and identifying the dominant causes is a relevant and challenging question but is hardly related to the research questions of this article. Therefore, in our study, we are not trying this; instead, we refer to the description of the different regional simulations published earlier. We touch briefly upon this, when discussing the different cases.

In section 3 we discuss the skill of a series of regionalizations obtained through dynamical downscaling—in Central Siberia, the Bohai Sea and the Yellow Sea, Southwestern Africa, and the South Atlantic (see Figure 1).

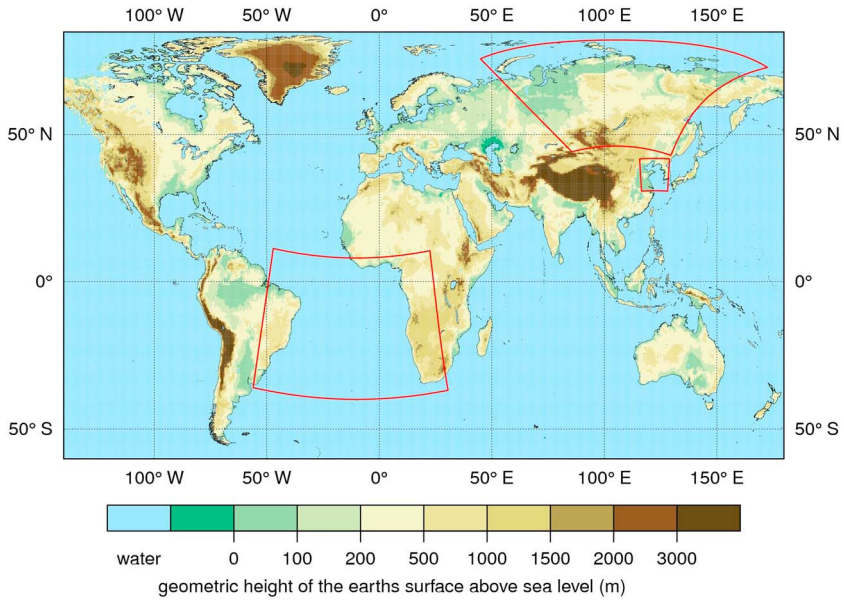

Figure 1. Regions for which regional downscaling products were generated: Bohai Sea and Yellow Sea region, Central Siberia, Southwest Africa/Southern Atlantic, and the entire domain for the global downscaling.

These three cases have been compiled in three extensive studies employing large-scale constraining in different regional atmospheric models but with different setups, the choices of which were related to the application, purpose of the studies, and computer resources at their time. Thus, our ensemble of cases is an "ensemble-of-opportunity," which has its merits because of the variety of setups. The end-result is that for the research question "Are regional analyses of weather in the past decades possible in data-sparse regions?" a positive answer is found, independently of the specifics of the setup.

These three regions have less good meteorological data coverage than other areas with traditionally denser station coverage. In one case, namely, Siberia, we demonstrate the limitations of the constraining, when the homogeneity and validity of the large-scale description of the reanalysis are compromised. In another case, the Yellow Sea, we demonstrate the additional skill of describing mesoscale phenomena such as vortex streets. In the third case, Southwestern Africa/South Atlantic, we analyze the added values in the marine near-surface wind field.

Finally, in section 4, we introduce a "global regionalization" effort, which is a global simulation within which the large-scales are constrained.

The overall "message" of this article is twofold: that skillful regional descriptions of multidecadal climate variability may be constructed in regions with little or no local data. Second, that global dynamical downscaling allows completing global reanalyses with consistent detail in all regions of the world.

2. Cases and Methods

Four different cases are considered in this study, three regional downscalings, and one global downscaling. For our three regional analyses we applied the nonhydrostatic regional climate model COnsortium for Small-scale MOdelling model in CLimate Model (COSMO-CLM) (CCLM) [*Rockel et al*., 2008b] using different sets of reanalyses as atmospheric driving fields. The global analysis was conducted by means of the global climate model European Centre/Hamburg version 6 (ECHAM6) [*Stevens et al*., 2013].

2.1. Bohai Sea and Yellow Sea

The conventional surface and upper air observations of pressure, temperature, wind, and the other atmospheric parameters are mainly distributed over developed and densely populated land areas. Observations over the marine regions, which typically include oceanographic buoy or vessel measurements, are much sparser spatially and temporally, such as the Chinese water areas [*Dow*, 2004; *Li*, 2010] According to National Climatic Data Center data set (https://gis.ncdc.noaa.gov/maps/ncei/cdo/hourly), there are only 15

coastal stations with observations spanning longer than 50 years around the Bohai Sea and Yellow Sea (BYS) (China: nine stations, North Korea: one station, Korea: five stations, while offshore observations are mostly available after 2000s [*Li*, 2010]. Available long-term global reanalysis, e.g., NCEP1, cannot effectively resolve mesoscale dynamics and also suffers from temporal inhomogeneity problems over East Asia prior to the late 1960s [*Yang et al*., 2002].

A grid resolution of 0.0625° was employed for downscaling over the BYS during 1979–2013. ERA-Interim reanalysis data were used as initial and boundary conditions and for large scale (>350 km**)** constraining of the horizontal wind fields above 850 hPa. There are 168 × 190 grid points in the longitudinal and latitudinal directions and 10 grid boxes as a sponge zone at the lateral boundary at each side.

The simulation data are accessible at the Climate and Environmental Retrieval and Archive (CERA) data bank of German Climate Computer Centre, via https://cera-www.dkrz.de/WDCC/ui/cerasearch/q?query=*:*&project_name_ss=coastDat-2%20%28coastDat-2%29.

The BYS region is dominated by the East Asian monsoon climate system. The simulation was run for obtaining a long-term atmospheric database to derive past and current climate statistics, including their variability, climatology, and extremes, to contribute to the assessment of climate change impact over the BYS areas. The high-resolution atmospheric data set is also vital in forcing ocean models and in applications such as potential wind energy assessments [*Li et al*., 2016a].

With advanced subgrid-scale parametrization and high-resolution local physiographic conditions, the RCM is expected to capture more realistic medium-scale processes than its forcing data set. Based on spatial filtering methods, the added value over the coastal areas of BYS proves to be highly related to better representation of medium-scale features by CCLM [*Li et al*., 2016b]. In detail, we presume that some orographic-related coastal mesoscale such as coastal atmospheric gravity waves, mountain gap winds, vortex streets, and even tropical cyclones may be key factors that contribute to the added value of CCLM in coastal areas of the BYS. It has been partially demonstrated based on the case studies in *Li* [2017]. Furthermore, the occurrence frequency and strength of those mesoscale features captured by CCLM contribute to the seasonality of added value. However, distinguishing contributions of different mechanisms to added value would be challenging and would need much more efforts.

2.2. Central Siberia

For central Siberia, a vast region that extends from the polar to temperate latitude in Siberia, regional detailed snow cover characteristics as SWE is restricted because of the lack of reliable observational data [*Ge and Gong*, 2008; *Bulygina et al*., 2011]. The meteorological network is sparse, and data records suffer from incomplete data records, inhomogeneous measurement techniques, limited length, or unevenly distributed stations [*Adam and Lettenmaier*, 2008; *Groisman and Rankova*, 2001; *Khan et al*., 2008; *Serreze et al*., 2003]. After the disintegration of the Soviet Union, many stations were closed [*Adam and Lettenmaier*, 2008; *Khan et al*., 2008; *Serreze et al*., 2003] or were not accessible in the late 1980s and early 1990s.

We consider this region by running a regional atmospheric model with a grid resolution of 55 km. The model was forced by NCEP1 and ERA-40 reanalyses. The downscaling was done for 1948–2010 with NCEP1 forcing and, in a second simulation, for 1959–2001 with ERA-40 forcing [*Klehmet and Rockel*, 2015]. In both cases we applied spectral nudging for large-scale wind fields greater than 1000 km and above 850 hPa. The simulation data are stored in the CERA-System, doi:10.1594/WDCC/COSMO-CLM_siberia. The simulation data are stored in the CERA-System, doi:10.1594/WDCC/COSMO-CLM_siberia.

In general, downscaling results depend on the quality of the atmospheric large-scale driving data providing lateral boundary condition [*Diaconescu and Laprise*, 2013; *Laprise et al*., 2012; *Rockel et al*., 2008b; *Wu et al*., 2005]. Erroneous atmospheric driving data may affect the downscaling result. This occurred over Mongolia in summer during 1959–1967 when NCEP1 suffered from a significant error in the description of the large-scale atmospheric state [*Inoue and Matsumoto*, 2004; *Yang et al*., 2002]. *Inoue and Matsumoto* [2004] showed a statistically significant increase of 7 hPa in sea level pressure between 1980–1999 and 1960–1979. This inconsistency was denoted as" psfc problem" [*Inoue and Matsumoto*, 2004; *Yang et al*., 2002] and originated in the omission of direct surface and sea level pressure measurements when the pressure was below 1000 hPa (refer to http://www.emc.ncep.noaa.gov/gmb/bkistler/psfc/psfc.html). The problem partly prevailed even for the period until 1979 [*Huang et al*., 2011].

This misrepresentation of the large-scale states propagated to the RCM so that these years had to be removed from the regional downscaling product driven with NCEP1 for that domain. However, for the Arctic and central Siberian regions, temporal consistency is given and the regional analysis can provide regional detailed climate information back to 1948 [*Klehmet*, 2014]—under the assumption that the large-scale description of NCEP1 in this part of the world is homogeneous. The motivation for the regional climate reconstruction was to assess snow cover changes at regional detail as snow cover is one important cryosphere variable shaping the land surface and thus the climate of Siberia.

2.3. Southwest Africa and Southern Atlantic

The understanding of the variability of coastal upwelling dynamics at the South African coast requires the analysis of surface wind data with high spatial resolution [*Small et al*., 2015]. On the one hand, regional ocean models require high-resolution forcing to realistically simulate coastal upwelling. Additionally, the temporal variability of the structure and amplitude small-scale atmospheric eddies may be different from the variations of the slowly varying large-scale atmospheric circulation.

Observational data are sparse over the African continent [*Ambrosino and Chandler*, 2013] and, in general, over the southern hemisphere [*Sterl*, 2004]. Therefore, reanalysis data sets are used instead. Nevertheless, these reanalysis data sets can contain inhomogeneities due to adjusting the sparse data coverage over regions like the African continent [*Ambrosino and Chandler*, 2013]. In particular, the inclusion of satellite data from 1979 onward has caused discontinuities in the resulting reanalysis data sets [*Sterl*, 2004]. In particular, there are very little information on surface winds along the Southern African upwelling regions, with only a few stations proving decadelong time series of monthly mean wind speed and direction [*Hagemann*, 2008]. The wind data available from satellite retrievals only cover the last 15 years, and they are inadequate to analyze the low-frequency variations of coastal upwelling intensity. The purpose of this simulation was to construct a more adequate surface forcing to drive a regional ocean model simulation over several decades that could more realistically represent coastal upwelling and its decadal variability.

We attempted a regional analysis by employing a dynamical downscaling effort with a horizontal grid resolution of about 16 km for 1979–2012, forced by ERA-Interim reanalysis. Spectral nudging was used for constraining the simulation on large scales of about 1000 km and more. The simulation data are stored in the HPSS doku of the DKRZ (German Climate Computing Center) https://www.dkrz.de/Nutzerportal-en/doku/hpss.

The simulation aimed primarily at describing realistically sea level pressure and wind conditions, because of their significance for the upwelling system and its changes. This model run focused on the Benguela upwelling region, located off the coasts of Angola, Namibia, and South Africa [*Tim et al*., 2015]. The data set also provides a high-resolution reconstruction of the climate over land areas of southwest Africa. This region encompasses quite different climate regimes and landscapes, ranging from the tropical climate of Angola, the subtropical deserts of Namibia and Botswana, to the South African regions, which are more affected by extratropical synoptic perturbations. The coastal zones of Namibia and South Africa are subject to particular meteorological conditions caused by upwelling cold water, which lead to frequent haze conditions along the coast, and create a sharp surface temperature contrast relative to landward areas.

2.4. Global Downscaling

A global description of past regional weather phenomena by constraining a global model with large-scale reanalyses has been suggested by *Yoshimura and Kanamitsu* [2008]. We repeated their effort for the period of 1948–2015 by feeding the large-scale atmospheric states given by NCEP1 reanalyses into the high-resolution climate model ECHAM6 (T255L95—horizontal fields are expanded into spherical harmonics up to total wave number 255, which amounts to a grid-point distance of about 55 km; the vertical is discretized into 95 vertical levels [*Schubert-Frisius et al*., 2017]). As in the regional cases, the spectral nudging technique was also employed here in this global dynamical downscaling process. The resulting data were stored at hourly interval with a spatial grid resolution of about 50 km. The data can be downloaded here: http://icdc.cen.uni-hamburg.de/1/daten/atmosphere/echam6-climate-reconstruction.html.

In all cases, the "spectral nudging" constraining [*von Storch et al*., 2000] is used; i.e., the models are integrated with an additional term which penalizes large-scale deviations from prescribed states given by some global reanalyses such as NCEP1 or ERA-interim.

Next we describe our choice to determine if an added value has been achieved in the regional and global cases, namely, the reduction of error variance.

We measure the added value by the modified Brier Skill Score (BSS) [*Winterfeldt et al.*, 2011], which describes the improvement by the downscaled quantity x_D over a "competitor" x_C in reproducing some "truth" x_O

$$\mathrm{BSS} = \begin{cases} 1 - d^2(x_D, x_O)/d^2(x_C, x_O) & \text{if } d^2(x_D, x_O) \leq d^2(x_C, x_O) \\ d^2(x_C, x_O)/d^2(x_D, x_O) - 1 & \text{if } d^2(x_D, x_O) > d^2(x_C, x_O) \end{cases}, \quad (1)$$

where $d^2(x_1, x_2)$ denotes the mean squared difference between the two fields x_1 and x_2.

In section 3 the BSS is calculated based on the downscaled product x_D relative to its driving reanalysis x_C using observations x_O as reference data.

In the BYS region the focus was on surface wind conditions. The quality of reconstructed surface wind speeds (1979–2013) and added value from dynamical downscaling to the forcing data set ERA-Interim was assessed against in situ observations and QuikSCAT wind data (see Appendix A1).

For Central Siberia, the BSS was calculated for the snow water equivalent (SWE) in January and April over the period of 1987–2010 of the downscaled data set relative to the SWE product in the ERA-Interim reanalysis. Satellite-derived SWE of European Space Agency (ESA) GlobSnow was used as observational reference data (see Appendix A2). Note, that the regional model was driven not with ERA-Interim but with NCEP1, which, however, provides no meaningful snow water equivalent.

For the Southwestern Africa and the South Atlantic region, we focus again on daily mean near-surface marine winds which are the main driver of the Benguela upwelling. We compare the skill of the downscaled daily wind speeds for the period of 2000 to 2009 relative to the driving ERA-Interim analyses. The observational truth x_O was taken to be the observational data set QuikSCAT (see Appendix A1).

For the global downscaling, the BSS was computed for 10 m wind speed for the decade 1999 (December) to 2009 (November). The quality of the global reconstruction in comparison to its forcing NCEP reanalyses was computed against ERA-Interim data, which served as a reference.

In section 4 we use the global downscaling as competitor x_C. In this way we determine for the three regional downscaling products, for the South Atlantic, Siberia, and the Yellow Sea, how similar they are compared to the global downscaling product.

3. Added Value of Regional Analyses and Global Regionalization

In this section, we evaluate the results of downscaling with observational data and compare them with their driving reanalysis.

3.1. Bohai Sea and Yellow Sea

High-resolution regional downscaling of surface winds proves to be realistic in resolving the regional wind characteristics over the BYS, based on statistical results using metrics such as bias, correlation coefficient, and root-mean-square error [*Li et al.*, 2016b]. The regional model has a smaller error variance than the forcing data set (indicated by a positive BSS) in terms of surface winds in the near coastal areas with complex coastlines and orography (Figure 2a); for strong wind speeds of 10.8–25 m/s (Figure 2b), the areas with positive BSS are even larger, including the Bohai Sea and the coastal and some offshore areas of the Yellow Sea. Thus, the downscaled product performs better than the forcing data set, which we call added value. Added value emerges in the coastal areas for all seasons; however, the added value is more widespread in summer and autumn than in winter and spring (not shown here).

With respect to mesoscale dynamical processes, the regional downscaling outperforms the forcing data set ERA-Interim in resolving fine temporal and spatial scales for phenomena such as tropical cyclones and vortex streets [*Li*, 2017]. In case of a vortex street downstream of Jeju Island (Figure 3), which generally forms when strong airstreams flow across the island in cold seasons, a strong wake with low wind speed is generated in the downwind path of the island in the regional downscaling product (Figure 3c), and then develops into a wave extending about 200 km downwind of the island (Figure 3d). In the ERA-Interim reanalysis wind fields

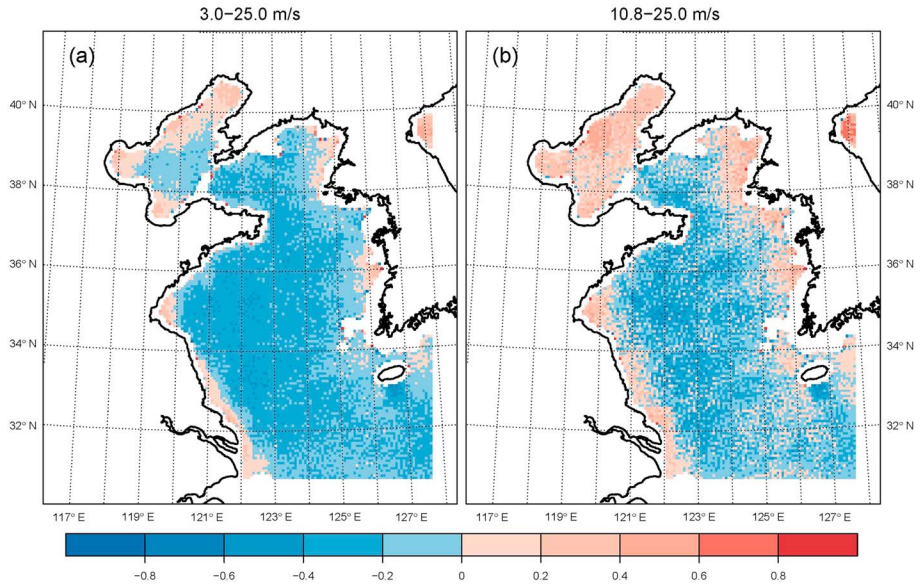

Figure 2. BSS for marine surface wind speeds of (a) 3–25 m/s and (b) 10.8–25 m/s over the Bohai and the Yellow Sea, comparing the downscaled product (with a regional model) and the driving ERA-Interim reanalysis. QuikSCAT wind data are used as "true" field. Positive values indicate a more realistic description by the downscaled product than by the driving reanalysis.

no sign of this vortex street is detected. For resolving the vortex structure in more detail even higher resolution than the 7 km grid used here is needed.

3.2. Central Siberia

Regional downscaling can add value to NCEP1 in reproducing snow water equivalents (SWE) as shown by *Klehmet et al.* [2013] for Siberia for the years 1987–2010. Dynamical downscaling of the atmospheric forcing fields of NCEP1 is usable to derive historical SWE fields with more realistic information than the driving reanalysis product itself can provide. In addition, the regional analysis is more homogeneous in terms of January SWE for the years 1987–2010 than the SWE product of ERA-Interim presenting spurious jumps in 2003 [*Klehmet et al.*, 2013]. This temporal inconsistency might be related to the geolocation errors that have affected the ERA-Interim snow analyses after July 2003, as stated in *Dee et al.* [2011].

The driving NCEP-reanalysis was inhomogeneous, with possibly erroneous data in the period from 1959 until 1967 and to a lesser extent until 1979 (see above in section 2); it suffered from another limitation, namely, that the SWE was set to a constant value of 30 mm [*Kanamitsu et al.*, 2002]. Thus, it makes little sense to calculate the BSS of the driving NCEP and the downscaled data (with GlobSnow as reference). Therefore, we compare the NCEP-downscaled SWE with the analyzed SWE of ERA-Interim and with ESA GlobSnow as observational reference (Figure 4).

It has to be emphasized that the BSS depends on the quality of observational reference data of ESA GlobSnow, which is also restricted due to its coarse patterns of SWE despite the 25 km spatial resolution [*Klehmet et al.*, 2013] caused by kriging interpolation methods, missing values in mountainous areas and water bodies and the tendency of underestimation of deep snowpack [*Takala et al.*, 2011]. Altogether this makes the assessment of the SWE simulation a bit difficult.

However, a comparison with in situ observations as, e.g., the Former Soviet Union Hydrological Snow Surveys (FSUHSS) for SWE would be problematic as well. SWE data of those transect measurements are seldom and not evenly distributed and ended in 1996 [*Krenke*, 2004; *Klehmet*, 2014]. Reliable in situ data of variables such as precipitation, snow depth, or SWE at high-latitudes are especially difficult to measure due to problems of gauge undercatch of wind-induced losses or redistribution [*Adam and Lettenmaier*, 2008; *Serreze et al.*, 2003]. Additionally, the results would be affected by the grid box versus station comparison; one grid box represents a mean area of ~2500 km^2. Therefore, we decided so stay with ESA GlobSnow as observational reference in order to have the assessment for the entire area keeping the limitations in mind.

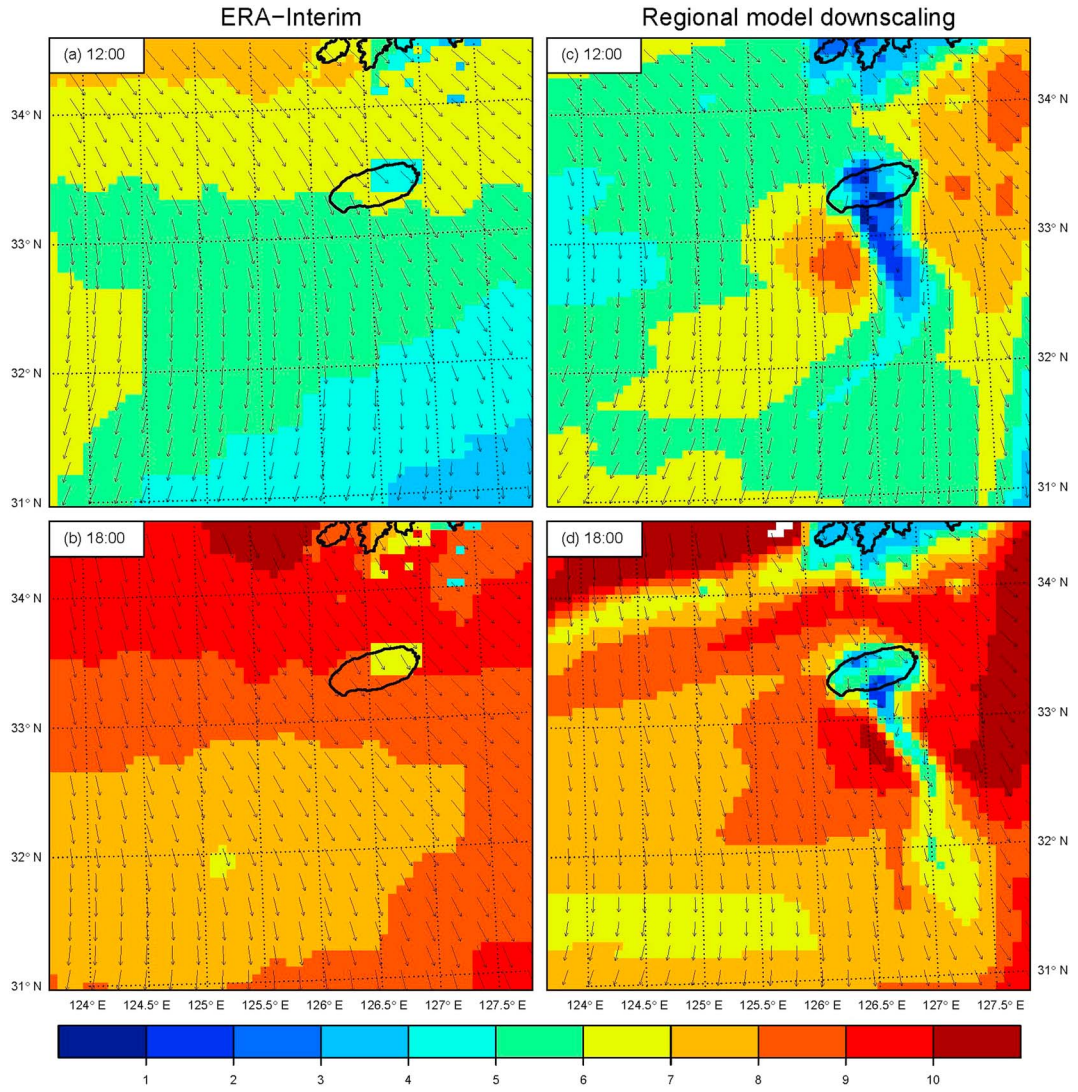

Figure 3. Spatial distributions of wind speed (m/s) and vectors around Jeju Island at 12:00 UTC and 18:00 UTC 17 January 1997 for (a and b) ERA-Interim reanalysis data and (c and d) the regional downscaling product.

Figure 4 illustrates that in some areas, ERA-Interim reproduces the GlobSnow data better than the downscaled data, but in others the opposite is true. The high positive values, e.g., in the central domain in January can be related to the overestimation of SWE in ERA-Interim when compared with GlobSnow. This was also evident when compared to transect measurements of the FSUHSS data [*Klehmet et al.*, 2013]. In contrast to April along the Central Siberian Plateau, here the downscaled product overestimates the SWE and ERA-Interim indicates better results. An explanation might be the delayed melting or poor representation of snow melting processes. It has to be noted that GlobSnow used snow depth observations provided by the ECMWF as first step input before the satellite radiometer measurements were taken into account [*Takala et al.*, 2011]. So the GlobSnow product and the SWE from ERA-Interim are not completely independent.

By and large, the two methods—namely, the analysis in the local data-driven ERA-Interim and the large-scale-driven CCLM downscaling—generate estimates of SWE of similar quality.

The exercise shows that the technique of dynamical downscaling of atmospheric forcing fields (e.g., pressure and wind) provided by NCEP1 can be used to add more realistic information than the reanalysis product itself presents. This is possible because of the model physics of the RCM and finer-resolved regional features, such as orography and land cover. Moreover, a more sophisticated snow model with the consideration of two snow layers and the usage of an increased soil column depth down to 92 m are important aspects in the

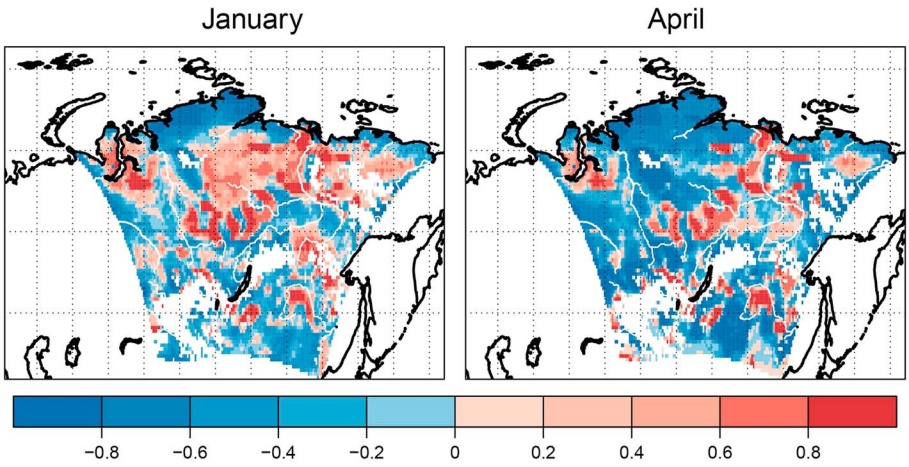

Figure 4. BSS for snow water equivalent in January and April in Central Siberia (1987–2010), comparing the downscaled product (with a regional model) and ERA-Interim reanalysis. As reference (truth) ESA GlobSnow is used. The positive values indicate a more realistic description of the downscaled product than of ERA-Interim. The white grid boxes within the model domain indicate missing values given by ESA GlobSnow. Note that the regional model was driven not with ERA-Interim but with NCEP, which, however, provides no meaningful snow water equivalent.

downscaling over Siberia [*Klehmet*, 2014]. We showed that the regional downscaling is comparable to the ERA-Interim product.

3.3. Southwest Africa and Southern Atlantic

Near-surface marine winds are the main drivers of coastal upwelling in the Benguela region. Therefore, we examine the downscaled near-surface daily mean wind speeds for the period December 1999 through November 2009 and compare their BSS-skill to that of the driving ERA-Interim analyses. As before, the data set QuikSCAT (Appendix A1) is taken as the observational truth. All data sets were interpolated to the CCLM grid's horizontal resolution of about 16 km before calculating the BSS.

The BSS is in most areas small, in some areas positive along the coastline and in the eastern equatorial Atlantic, but over large areas mainly in midmarine regions negative (Figure 5). This pattern demonstrates that the downscaling provides added value in physiographic structured areas, namely, in this case coastal areas, whereas in large areas without small-scale surface conditions, the regional model fails to add detail.

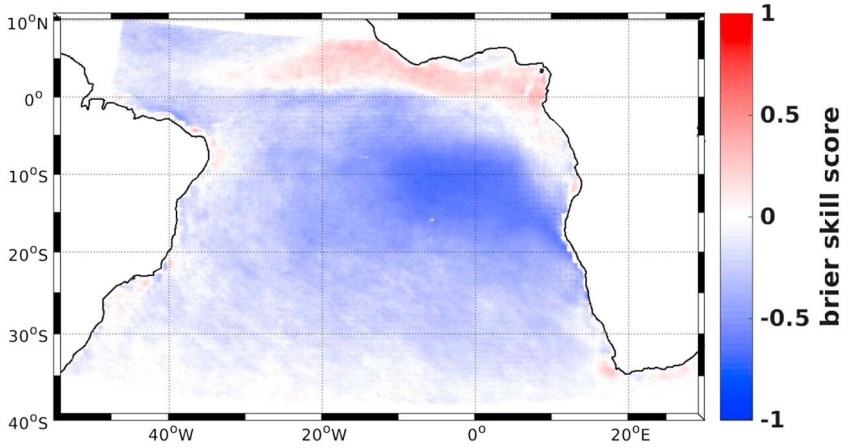

Figure 5. BSS for daily mean near-surface wind speed over Southwest Africa and the Southern Atlantic for the period December 1999 to November 2009 of the regional downscaling compared to the ERA-interim reanalysis data. QuikSCAT near-surface winds are used as reference. The red areas indicate a better performance of the downscaled data than the reanalysis data. Only daily mean wind speeds between 3 m/s and 25 m/s were included in this calculation.

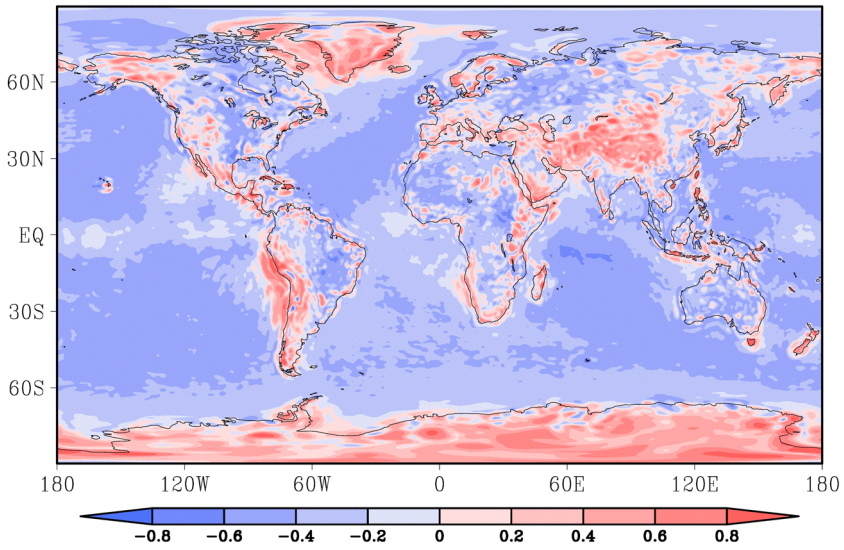

Figure 6. Global distribution of BSS, comparing the global downscaling data with the driving NCEP1 reanalysis, for 6 hourly 10 m wind speed for the decade 1999 (December) to 2009 (November). ERA-Interim reanalysis data are used as reference. The diurnal cycle has been taken out. Contour interval: 0.2.

However, there is a region in the Tropical South Atlantic where the skill of the regional simulations is markedly poorer than the ERA-Interim reanalysis. This region with lower skill of the regional model displays a higher interannual variability of the sea surface temperatures. We suggest that the poorer simulation of the daily wind speeds in this region may be related to a deficient model response to the tropical sea-surface-temperature variability.

3.4. Global Analysis

The global downscaling used NCEP1 as forcing data; as global reference we therefore employ ERA-Interim-data. The wind fields were constrained up to the total wave number 30 at levels above 750 hPa. The analysis presented here focuses on the time period of 1999–2009.

Figure 6 shows the BSS of 6 hourly wind speeds for spatial scales described by T31–T135 (at 45°N; this corresponds to a grid resolution of about 450 km–100 km) at a height of 10 m. (The spatial filtering was achieved by selecting the according wave numbers of the global model's spectral output.) Positive BSS values appear over large parts of South America, Antarctica, and Greenland. Added value on mesoscale and smaller scale can be found in regions of regional physiographic details, in particular, mountainous topography, islands, and coastal areas. However, negative values can be seen in regions with uniform surface conditions, such as central regions of the continents and over the open sea.

Most regional storms, like the synoptic-scale fall and winter storms in the midlatitudes (Europe) as well as hurricanes and typhoons in the lower latitudes are better reconstructed in the global downscaling data set compared to NCEP1 [*Schubert-Frisius et al.*, 2017], although their intensity often still lies below those of best track data. A case considered in more detail was the 2014 hurricane Gonzalo which underwent an extratropical transition process [*Feser et al.*, 2015].

4. Comparison of Regional and Global Analyses

In this section, we compare the regional downscaling simulations with the global downscaling product.

4.1. Bohai Sea and the Yellow Sea Region

Figure 7a illustrates that global ECHAM downscaling adds value to its forcing data set NCEP1 over the Bohai Sea and parts of the Yellow Sea coasts. There is more improvement for strong wind speeds (Figure 7b), indicated by areas with positive BSS.

Regional model downscaling with 55 km grid resolution rarely adds value to the global model downscaling product for near-surface wind speeds of 3–25 m/s over the BYS region, with BSS values mostly within

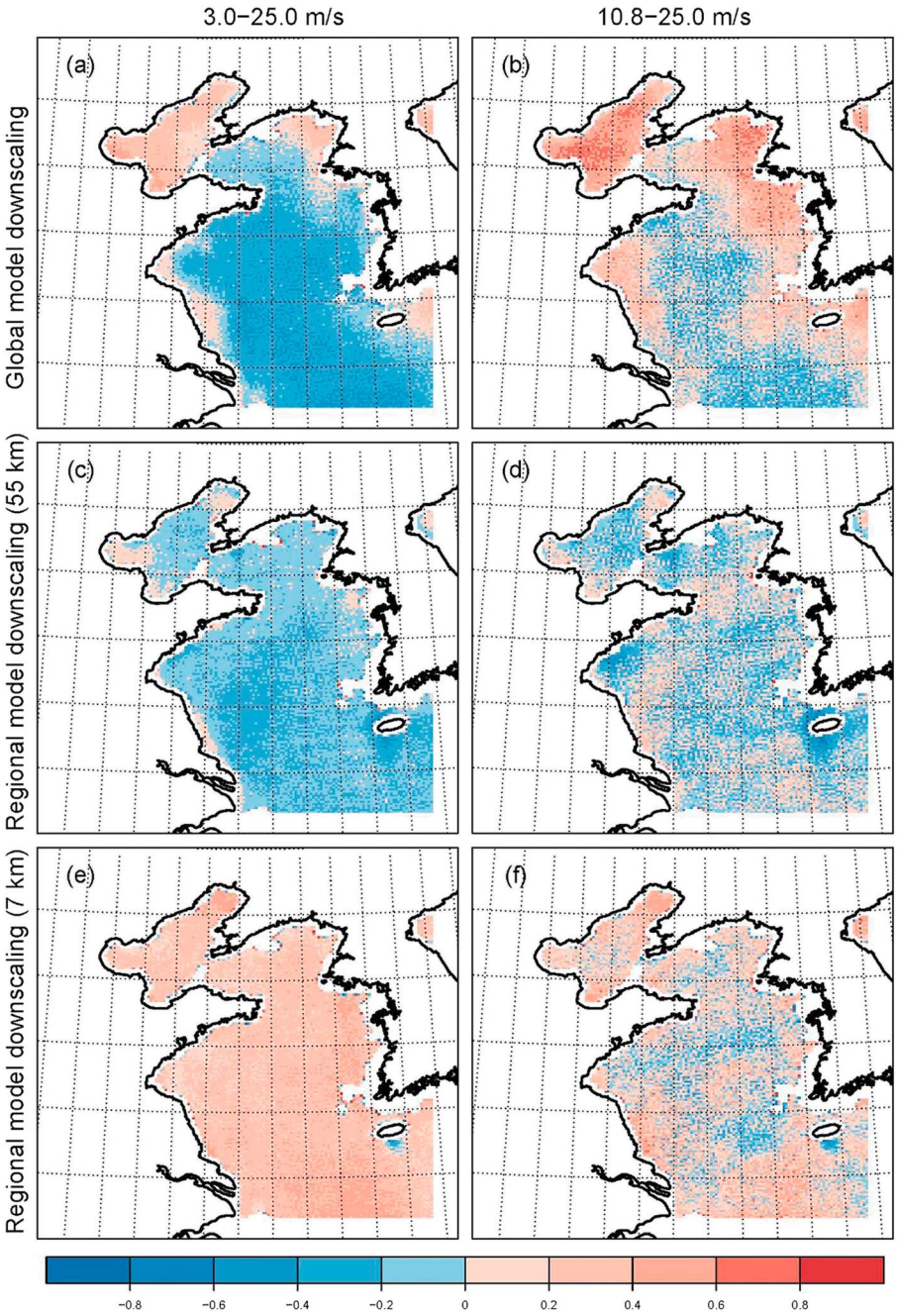

Figure 7. Brier Skill Scores over the period of December 1999 to November 2009 for marine surface wind speeds of (left column) 3–25 m/s and (right column) 10.8–25 m/s relative to observational reference data (truth) QuikSCAT. (top row) Comparison of the global downscaling product and the driving NCEP1. (middle row) Comparison of the regional (55 km) and the global downscaling product. (bottom row) Comparison of the regional (7 km) and the global downscaling product.

−0.2 (Figure 7c); however, it adds value to the global model downscaling for strong wind speeds of 10.8–25 m/s in some areas, which is, however, irregularly distributed (Figure 7d). The regional (55 km) and global downscaling products do not differ much, as the absolute BSS values are minor (Figures 7c and 7d).

A detail in Figures 7c–7f is that close to Jeju Island the BSS shows larger negative values indicating no added value (or rather worsening) for the higher-resolution regional downscaling compared to the global downscaling. This is not necessarily contradicting the findings in section 3 since the 12.5 km pixel

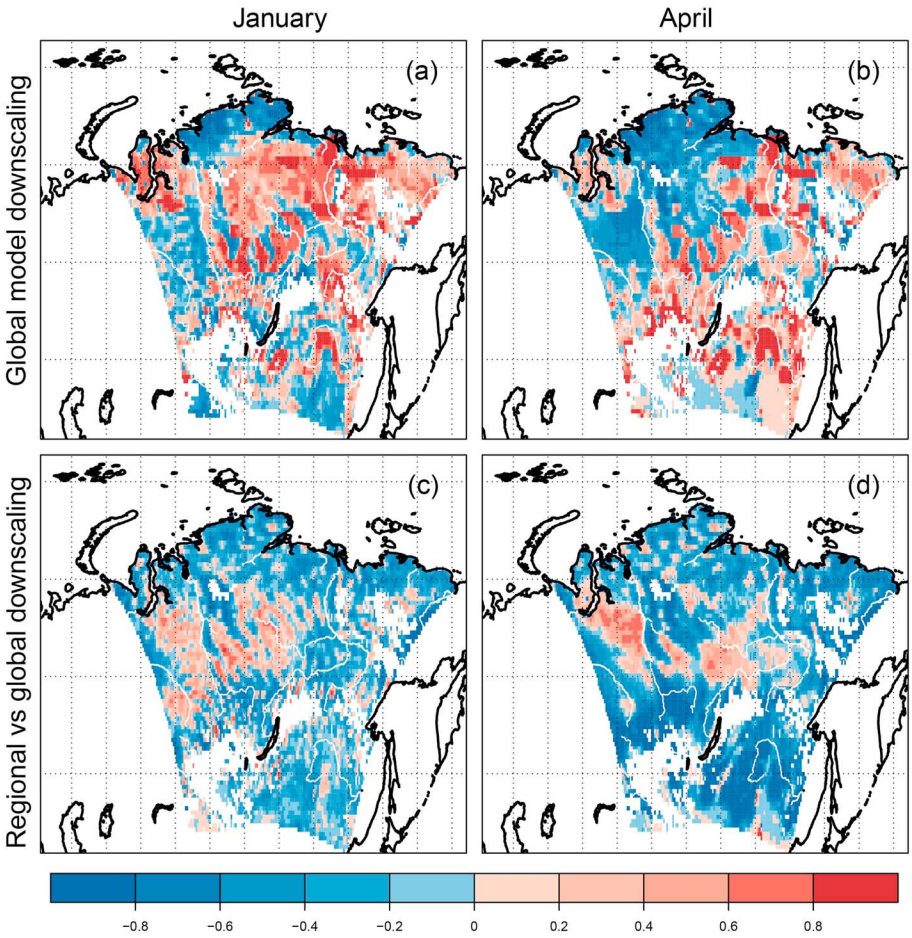

Figure 8. Monthly (January and April) BSS over the period of 1987–2010 for snow water equivalent (SWE) relative to ESA GlobSnow as observational reference data (truth) for Central Siberia in January and April. The white grid boxes indicate missing values given by ESA GlobSnow. (top) Comparison of the global downscaling product and ERA-Interim reanalysis (cf. Figure 4). Note that the downscaling was not forced with ERA-Interim, but NCEP, which, however, lacks useful information about the snow water equivalent(bottom) Comparison of the regional and the global downscaling product. The red areas indicate that the regional product compared is closer to observations than the global product.

resolution QuikSCAT data set is insufficient for capturing small-scale phenomena like the vortex streets excited by the island of Jeju.

The higher-resolution (7 km) regional downscaling product can add value to the global downscaling for almost the entire BYS region for wind speeds of 3–25 m/s. The skill of strong wind speeds of 10.8–25 m/s is of the same order, but the areas of positive added value are reduced (Figures 7e and 7f). The added value of the 7 km regional downscaling product compared to the global downscaling may benefit not only from its high resolution but also from its different driving data set, as the 7 km regional downscaling product is driven by ERA-Interim reanalysis, while the 55 km downscaling and the global downscaling products use NCEP1 reanalysis.

4.2. Central Siberia

The BSS calculated for the global downscaling product and the ERA-Interim reanalysis with ESA GlobSnow as reference (Figure 8) is mostly similar to the distribution obtained for the regional downscaling (see above, Figure 4). In January, the high-resolution global model returns a better regionalization than the regional model in terms of SWE having a larger spatial extent of positive BSS especially south of 50°N.

When the regional and the global downscaling are compared directly, using GlobSnow as reference, mostly negative values of the BSS are presented during January and April (Figures 8c and 8d), indicating a superior performance of the global downscaling product.

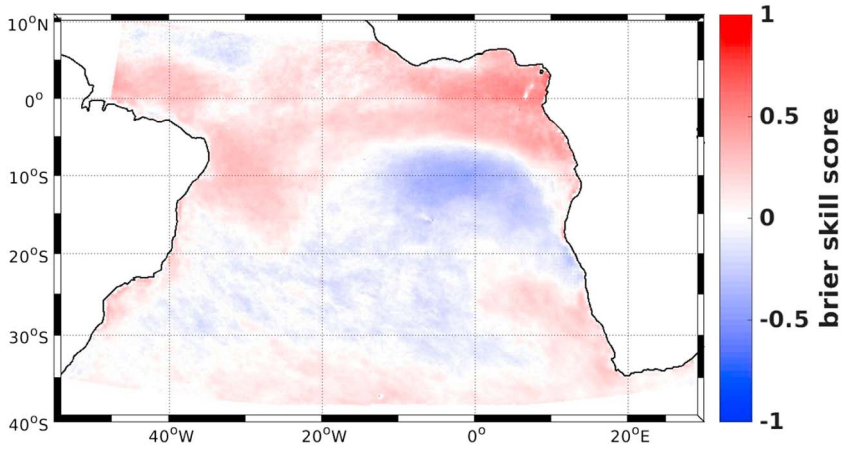

Figure 9. BSS comparing the regional (CCLM_16 km) and global (ECHAM_50 km) downscaling products over Southwest Africa and the Southern Atlantic for near-surface daily mean wind speeds. As reference, QuikScat analysis is used. Time window: December 1999 to November 2009. The red shades represent that the regional model is closer to the satellite data, whereas the blue shades show that the global model is more realistic. Only daily mean wind speeds between 3 m/s and 25 m/s were included in this calculation.

4.3. Southwest Africa and Southern Atlantic

The comparison of the regional downscaling and the global downscaling reveals that the former is returning in some regions more realistic values in terms of daily mean wind speed. Figure 9 compares the two downscaling products, with red colors indicating a better performance of the regional product and blue colors a better performance of the global product. Particularly, in the coastal regions and over the equatorial Atlantic, the regional model generates more realistic mean winds, while in the zone of high sea surface temperature variability (in the Tropical South Atlantic around 12°S), the global model performs better. There are many possible reasons for these deviations between the regional and the global models. The stratocumulus cloud decks over the Namibian upwelling area might cause the discrepancy between the two simulations.

Despite these regional differences, the two methods seem to generate comparable results (with low BBS values and blue and red areas of a similar size in Figure 9) for the case of near-surface wind over the South Atlantic.

5. Discussion

Dynamical downscaling by constraining dynamical models on large spatial scales is by now a well-established method. The idea of applying this concept not only in regional models but also in global models was introduced more recently, even if it was an obvious extension.

Downscaling serves two major purposes. One is a reconstruction of the past weather stream in a region. The second is the construction of consistent regional manifestations of scenarios of regional climate change. Here we have dealt exclusively with the former. We are looking for long-term homogeneity of the product: if amount and quality of evidence are changing over time, then the request for homogeneity requires to disregard those components which monitor more detail over time, because a change in such details in the analysis cannot be related to the availability of better evidence or real change. Thus, a homogeneous analysis must accept lowest data quality during the analysis time—or shorten the analysis time window. The downscaled product will almost always be less accurate than efforts for the last years and decades, also when compared to global high-resolution but shorter reanalyses. When interested in weather states including hazards and change, after 1979, the improved ERA-Interim is an adequate forcing field, but when multidecadal variability is of interest, then a downscaling of NCEP1, beginning in 1958 or even 1948, is an appropriate choice.

An alternative is of course a regular regional analysis making use of quality controlled and homogenized local data (such as North American Regional Reanalysis [*Mesinger et al.*, 2006] or COSMO-REA6 [*Bollmeyer et al.*, 2015]. The problem with reanalysis, both regional and global, is that the driving data—namely, the local observations—are inhomogeneous in quality and density, so that smaller scales will vary not because of

changing weather statistics but because of procedural changes [e.g., *Compo et al*., 2011]. But we expect that more and better regional reanalysis will be constructed in the future.

However, for regions and times when hardly any local data exist, this approach cannot be pursued. Then, only our approach of processing the large-scale descriptions which are believed to be constructed homogeneously with global reanalyses can be used. Our results demonstrate that this method of constructing homogenous analysis describing regional effects also works in data-sparse regions. Climate statistics of variables obtained from our approach such as coastal surface wind and snow water equivalent can add value to their forcing data sets; some orographic-related meso-scale features are better described in constrained RCMs than in the forcing reanalyses.

A key problem is then to determine which large scales are considered homogeneous, and which are not. So far, no robust methodology for determining these scales has been suggested, and the presently used choices are made ad-hoc.

In our study, we have used "cases of opportunity," i.e., real cases, where regional analyses were constructed in regions with sparse data coverage (in time and space). Therefore, the data for the comparison of global and regional downscaling are taken from the work of different scientists with different scientific aims. This makes the data sets not as consistent as they ideally could be. Different driving global reanalysis and physical parameterizations have certainly an influence on the comparison. Therefore, the different cases are compared qualitatively and less so quantitatively. A more consistent way would be to use the same global reanalysis data and physical parameterizations for each model and simulation. However, models are generally setup to get the best performance; the optimal configuration will vary depending on the geographical region of interest. An equal setup may not give a fair comparison between the models.

Currently, in the process of considering smaller and smaller scales, the regions covered by regional climate models often become smaller [e.g., *Prein et al*., 2015]; then the significance of employing a spectral nudging method diminishes [*Schaaf et al*., 2017]. However, if models covering the globe or large regions, such as continents, are used for downscaling, the spectral nudging component will remain a necessary tool for allowing the large-scale component of global reanalyses to constrain the model trajectory.

The two products generated on the 55 km grid by the regional CCLM and by the global ECHAM6 have similar spatial resolutions, and they seem to have a comparable skill. One difference is that the global model needed stronger spectral nudging than the regional models. A plausible reason would be that the regional models are also constrained by the lateral boundary values.

The similar skills indicate that once a global downscaling has been done, with the higher computational burden, additional simulations with regional models with similar grid resolution are not needed. This represents a significant advantage—that all regions are done at the same time and in a comparable setup—so that we may see this approach as the standard, when moderate regional resolution is sought. An advantage of this format is that it would allow for consistent comparisons across various regional domains.

Conditional upon the availability of future computing resources, however, higher-resolution simulations, for instance allowing for explicitly modeled convection, will in the foreseeable future be done with regional models, which are computationally less demanding than global models.

The different data sets presented in this article are archived and may be freely used for scientific purposes. Of course, before application, a careful analysis of the quality for the intended application is needed, as sometimes temporal inconsistencies in the description of large-scale driving states prevail.

Appendix

A1. QuikSCAT

In order to assess the added value of regional climate modeling on marine surface wind, the latest reprocessed version 3 of the QuikSCAT Level 2B wind data was used as truth during December 1999 to November 2009 (accessible via ftp://podaac-ftp.jpl.nasa.gov/allData/quikscat/L2B12/v3/). The data were provided on a nonuniform grid within the swath at a 12.5 km pixel resolution. We co-located the QuikSCAT swath data to the model grid, i.e., 7 km resolution in case of the BYS region [see *Li et al*., 2016b].

QuikSCAT measurements below 3 or over 25 m/s were excluded due to their limited quality [e.g., *Hoffman and Leidner*, 2005]. The product is generally of good quality and useful for comparisons [*Fore et al*., 2014].

ERA-Interim reanalysis and QuikSCAT data are not independent data sets, as the latter was assimilated in the former after being aggregated at 50 km resolution [*Dee et al*., 2011] (this is not so for NCEP1). Therefore, the high agreement between QuikSCAT and ERA-Interim in most areas is to be expected, and determining added value by regional climate modeling by comparing with ERA-Interim as reference data set may be a bit unfair. However, the features of 50 km and less are lost when the QuikSCAT data are introduced into the ERA-Interim reanalysis, making the high-resolution QuikSCAT data suitable for field comparisons of small-scale features.

A2. ESA GlobSnow

The "snow water equivalent" (SWE) is a good parameter for characterizing snow conditions. We use the gridded, 25 km resolved satellite-derived SWE data set as observational reference provided by the European Space Agency (ESA) Data User Element GlobSnow project (http://www.globsnow.info/). The GlobSnow SWE product was derived by combining an assimilation scheme using passive satellite microwave radiometer data and in situ measurements of snow depth (collected by ECMWF from national observing networks) together with a time series melt detection algorithm [*Pulliainen*, 2006; *Takala et al*., 2009]. For the interpretation of passive microwave data and the calculation of SWE estimates the Helsinki University of Technology semiempirical snow emission model was applied [*Takala et al*., 2011]. The Globsnow data contains radiometer information of scanning multichannel microwave radiometer for 1979–1987, Special Sensor Microwave/Imager for 1987–2002 and Advanced Microwave Scanning Radiometer–EOS for 2003–2009. Wet snow and vegetation may have an effect on the accuracy of the data. Mountain areas were masked out because of strong orographic complexity [*Takala et al*., 2011]. Here we use the daily L3A-product (v1.2). The data coverage of that data set is best for 1987–2010 for January and April. These 2 months represent months of snow accumulation and the beginning of snowmelt in the southern regions.

Acknowledgments

The work was partly supported through the Cluster of Excellence "CliSAP" (EXC177), Universität Hamburg, funded through the German Research Foundation (DFG). It is a contribution to the Helmholtz Climate Initiative REKLIM (Regional Climate Change), a joint research project of the Helmholtz Association of German research centers (HGF). The CCLM is the community model of the German climate research (www.clm-community.eu). The German Climate Computing Center (DKRZ) provided the computer hardware for the regional and global climate model simulations. The simulation data are accessible at the German Climate Computing center (DKRZ): the BYS data via https://cera-www.dkrz.de/WDCC/ui/cerasearch/q?query=*:*&project_name_ss=coastDat-2%20%28coastDat-2%29; the Siberian data at doi:10.1594/WDCC/COSMO-CLM_siberia; the South Atlantic data at https://www.dkrz.de/Nutzerportal-en/doku/hpss; and the global simulations at http://icdc.cen.uni-hamburg.de/1/daten/atmosphere/echam6-climate-reconstruction.html. Sources for observational data are listed in the text and in Appendix A.

References

Adam, J. C., and D. P. Lettenmaier (2008), Application of new precipitation and reconstructed streamflow products to streamflow trend attribution in northern Eurasia, *J. Clim.*, *21*, 1807–1828.

Ambrosino, C., and R. E. Chandler (2013), A nonparametric approach to the removal of documented inhomogeneities in climate time series, *J. Appl. Meteorol. Climatol.*, *52*(5), 1139–1146.

Ban, N., J. Schmidli, and C. Schär (2014), Evaluation of the convection-resolving regional climate modeling approach in decade-long simulations, *J. Geophys. Res. Atmos.*, *119*, 7889–7907, doi:10.1002/2014JD021478.

Barcikowska, M., F. Feser, W. Zhang, and W. Mei (2017), Changes in intense tropical cyclone activity for the western North Pacific during the last decades derived from a regional climate model simulation, *Clim. Dyn.*, doi:10.1007/s00382-016-3420-0.

Berg, P., R. Döscher, and T. Koenigk (2013), Impacts of using spectral nudging on regional climate model RCA4 simulations of the Arctic, *Geosci. Model Dev.*, *6*, 849–859, doi:10.5194/gmd-6-849-2013.

Bollmeyer, C., et al. (2015), Towards a high-resolution regional reanalysis for the European CORDEX domain: High-Resolution Regional Reanalysis for the European CORDEX Domain, *Q. J. R. Meteorol. Soc.*, *141*, 1–15, doi:10.1002/qj.2486.

Bulygina, O. N., P. Y. Groisman, V. N. Razuvaev, and N. N. Korshunova (2011), Changes in snow cover characteristics over Northern Eurasia since 1966, *Environ. Res. Lett.*, *6*, 045204. [Available at http://stacks.iop.org/1748-9326/6/i=4/a=045204.]

Cavicchia, L., and H. von Storch (2011), The simulation of medicanes in a high-resolution regional climate model, *Clim. Dyn.*, *39*, 2273–2290, doi:10.1007/s00382-011-1220-0.

Chan, S. C., E. J. Kendon, H. J. Fowler, S. Blenkinsop, N. M. Roberts, and C. A. T. Ferro (2014), The value of high-resolution Met Office regional climate models in the simulation of multihourly precipitation extremes, *J. Clim.*, *27*, 6155–6174, doi:10.1175/jcli-d-13-00723.1.

Choi, S.-J., and D.-K. Lee (2016), Impact of spectral nudging on the downscaling of tropical cyclones in regional climate simulations, *Adv. Atmos. Sci.*, *33*, 730–742, doi:10.1007/s00376-016-5061-y.

Compo, G. P., et al. (2011), The Twentieth Century Reanalysis Project, *Q. J. R. Meteorol. Soc.*, *137*, 1–28, doi:10.1002/qj.776.

Dahlgren, P., T. Landelius, P. Kållberg, and S. Gollvik (2016), A high-resolution regional reanalysis for Europe. Part 1: Three-dimensional reanalysis with the regional HIgh-Resolution Limited-Area Model (HIRLAM), *Q. J. R. Meteorol. Soc.*, *142*, 2119–2131.

Dee, D. P., et al. (2011), The ERA-Interim reanalysis: Configuration and performance of the data assimilation system, *Q. J. R. Meteorol. Soc.*, *137*, 553–597, doi:10.1002/qj.828.

Diaconescu, E. P., and R. Laprise (2013), Can added value be expected in RCM-simulated large scales?, *Clim. Dyn.*, *41*, 1769–1800, doi:10.1007/s00382-012-1649-9.

Di Luca, A., R. de Elía, and R. Laprise (2012), Potential for added value in precipitation simulated by high-resolution nested regional climate models and observations, *Clim. Dyn.*, *38*, 1229–1247, doi:10.1007/s00382-011-1068-3.

Di Luca, A., R. de Elía, and R. Laprise (2015), Challenges in the quest for added value of regional climate dynamical downscaling, *Curr. Clim. Change Rep.*, *1*, 10–21.

Donat, M. G., J. Sillmann, S. Wild, L. V. Alexander, T. Lippmann, and F. W. Zwiers (2014), Consistency of temperature and precipitation extremes across various global gridded in situ and reanalysis datasets*, *J. Clim.*, *27*, 5019–5035, doi:10.1175/jcli-d-13-00405.1.

Dosio, A., H.-J. Panitz, M. Schubert-Frisius, and D. Lüthi (2015), Dynamical downscaling of CMIP5 global circulation models over CORDEX-Africa with COSMO-CLM: Evaluation over the present climate and analysis of the added value, *Clim. Dyn.*, *44*, 2637–2661, doi:10.1007/s00382-014-2262-x.

Dow, G., (2004), Developments in observational requirements for global numerical weather prediction, Master thesis, 107 pp., Univ. of Reading, U. K.

Feldmann, H., B. Früh, G. Schädler, H.-J. Panitz, K. Keuler, D. Jacob, and P. Lorenz (2008), Evaluation of the precipitation for South-western Germany from high resolution simulations with regional climate models, *Meteorol. Z.*, *17*, 455–465, doi:10.1127/0941-2948/2008/0295.

Feser, F., and M. Barcikowska (2012), The influence of spectral nudging on typhoon formation in regional climate models, *Environ. Res. Lett.*, *7*, 014024, doi:10.1088/1748-9326/7/1/014024.

Feser, F., M. Barcikowska, S. Haeseler, C. Lefebvre, M. Schubert-Frisius, M. Stendel, H. von Storch, and M. Zahn (2015), Hurricane Gonzalo and its extratropical transition to a strong European storm. [in "Explaining extreme events of 2014 from a climate perspective"], *Bull. Am. Meteorol. Soc.*, *96*(12), S51–S55.

Feser, F., B. Rockel, H. von Storch, J. Winterfeldt, and M. Zahn (2011), Regional climate models add value to global model data: A review and selected examples, *Bull. Am. Meteorol. Soc.*, *92*, 1181–1192.

Feser, F., and H. von Storch (2008a), Regional modelling of the western Pacific typhoon season 2004, *Meteorol. Z.*, *17*(4), 519–528.

Feser, F., and H. von Storch (2008b), A dynamical downscaling case study for typhoons in Southeast Asia using a regional climate model, *Mon. Weather Rev.*, *136*, 1806–1815, doi:10.1175/2007mwr2207.1.

Fore, A. G., B. W. Stiles, A. H. Chau, B. A. Williams, R. S. Dunbar, and E. Rodríguez (2014), Point-wise wind retrieval and ambiguity removal improvements for the QuikSCAT climatological data set, *IEEE Trans. Geosci. Remote Sens.*, *52*(1), 51C59, doi:10.1109/TGRS.2012.2235843.

Ge, Y., and G. Gong (2008), Observed inconsistencies between snow extent and snow depth variability at regional/continental scales, *J. Clim.*, *21*, 1066–1082, doi:10.1175/2007JCLI1829.1.

Geyer, B. (2013), High resolution atmospheric reconstruction for Europe 1948–2012: coastDat2, *Earth Syst. Sci. Data Discuss.*, *6*, 779–809, doi:10.5194/essdd-6-779-2013.

Geyer, B., R. Weisse, P. Bisling, and J. Winterfeldt (2015), Climatology of North Sea wind energy derived from a model hindcast for 1958–2012, *J. Wind Eng. Ind. Aerodyn.*, *147*, 18–29, doi:10.1016/j.jweia.2015.09.005.

Groisman, P. Y., and E. Y. Rankova (2001), Precipitation trends over the Russian permafrostfree zone: Removing the artifacts of pre-processing, *Int. J. Climatol.*, *21*, 657–678, doi:10.1002/joc.627.

Hagemann, K. (2008), Mesoscale wind atlas of South Africa (doctoral dissertation, Univ. of Cape Town). [Available at http://open.uct.ac.za/handle/11427/4858.]

Hamdi, R., H. Van de Vyver, R. De Troch, and P. Termonia (2013), Assessment of three dynamical urban climate downscaling methods: Brussels's future urban heat island under an A1B emission scenario, *Int. J. Climatol.*, *34*, 978–999, doi:10.1002/joc.3734.

Heikkilä, U., A. Sandvik, and A. Sorteberg (2011), Dynamical downscaling of ERA-40 in complex terrain using the WRF regional climate model, *Clim. Dyn.*, *37*, 1551–1564.

Hoffman, R. N., and S. M. Leidner (2005), An introduction to the near–real–time QuikSCAT data, *Weather Forecasting*, *20*, 476–493, doi:10.1175/WAF841.1.

Huang, W.-R., S.-Y. Wang, and J. C. L. Chan (2011), Discrepancies between global reanalyses and observations in the interdecadal variations of Southeast Asian cold surge, *Int. J. Climatol.*, *31*, 2272–2280, doi:10.1002/joc.2234.

Inoue, T., and J. Matsumoto (2004), A comparison of summer sea level pressure over east Eurasia between NCEP-NCAR reanalysis and ERA-40 for the period 1960–99, *J. Meteorol. Soc. Jpn.*, *82*, 951–958, doi:10.2151/jmsj.2004.951.

Kalnay, E., et al. (1996), The NCEP/NCAR 40-Year Reanalysis Project, *Bull. Am. Meteorol. Soc.*, *77*, 437–471, doi:10.1175/1520-0477(1996)077<0437:TNYRP>2.0.CO;2.

Kanamitsu, M., W. Ebisuzaki, J. Woollen, S.-K. Yang, J. J. Hnilo, M. Fiorino, and G. L. Potter (2002), NCEP–DOE AMIP-II Reanalysis (R-2), *Bull. Am. Meteorol. Soc.*, *83*, 1631–1643, doi:10.1175/BAMS-83-11-1631.

Karl, T. R., R. G. Quayle, and P. Y. Groisman (1993), Detecting climate variations and change: New challenges for observing and data management systems, *J. Clim.*, *6*, 1481–1494, doi:10.1175/1520-0442(1993)006<1481:DCVACN>2.0.CO;2.

Khan, V., L. Holko, K. Rubinstein, and M. Breiling (2008), Snow cover characteristics over the main Russian River basins as represented by Reanalyses and measured data, *J. Appl. Meteorol. Climatol.*, *47*, 1819–1833, doi:10.1175/2007JAMC1626.1.

Kida, H., T. Koide, H. Sasaki, and M. Chiba (1991), A new approach to coupling a limited area model with a GCM for regional climate simulation, *J. Meteorol. Soc. Jpn.*, *69*, 723–728.

Kistler, R., et al. (2001), The NCEP/NCAR 50-year reanalysis, *Bull Am. Meteorol. Soc.*, *82*, 247–267.

Klehmet, K., and B. Rockel (2015), Regional climate model hindcasts for Siberia over the last decades based on the COSMO-CLM model driven by NCEP1 and ERA-40, run by Helmholtz-Zentrum Geesthacht, *WDCC at DKRZ*, doi:10.1594/WDCC/COSMO-CLM_siberia.

Klehmet, K., B. Geyer, and B. Rockel (2013), A regional climate model hindcast for Siberia: Analysis of snow water equivalent, *Cryosphere*, *7*, 1017–1034, doi:10.5194/tc-7-1017-2013.

Klehmet, K. (2014), A model-based reconstruction of recent Siberian climate - focusing on snow cover, Dissertation, Univ. of Hamburg.

Kobayashi, S., et al. (2015), The JRA-55 Reanalysis: General specifications and basic characteristics, *J. Meteorol. Soc. Jpn. Ser II*, *93*, 5–48, doi:10.2151/jmsj.2015-001.

Kotlarski, S., et al. (2014), Regional climate modeling on European scales: A joint standard evaluation of the EURO-CORDEX RCM ensemble, *Geosci. Model Dev.*, *7*, 1297–1333.

Krenke, A. (2004), Former Soviet Union hydrological snow surveys, 1966–1996., Tech. rep., National Snow and Ice Data Center/World Data Center for Glaciology, Boulder, Colo.

Krueger, O., F. Feser, L. Bärring, E. Kaas, T. Schmith, H. Tuomenvirta, and H. von Storch (2014), Comment on "Trends and low frequency variability of extra-tropical cyclone activity in the ensemble of twentieth century reanalysis" by Xiaolan L. Wang, Y. Feng, G. P. Compo, V. R. Swail, F. W. Zwiers, R. J. Allan, and P. D. Sardeshmukh, climate dynamics, 2012, *Clim. Dyn.*, *42*, 1127–1128, doi:10.1007/s00382-013-1814-9.

Krueger, O., F. Schenk, F. Feser, and R. Weisse (2013), Inconsistencies between long-term trends in storminess derived from the 20CR reanalysis and observations, *J. Clim.*, *26*, 868–874, doi:10.1175/JCLI-D-12-00309.1.

Laprise, R., et al. (2012), Considerations of domain size and large-scale driving for nested regional climate models: Impact on internal variability and ability at developing small-scale details, in *Climate Change*, edited by A. Berger, F. Mesinger, and D. Sijacki, pp. 181–199, Springer, Vienna.

Larsén, X. G., and J. Mann (2009), Extreme winds from the NCEP/NCAR reanalysis data, *Wind Energy*, *12*, 556–573, doi:10.1002/we.318.

Li, D. (2017), Added value of high-resolution regional climate model: Selected cases over the Bohai Sea and Yellow Sea areas, *Int. J. Climatol.*, *37*, 169–179, doi:10.1002/joc.4695.

Li, D., B. Geyer, and P. Bisling (2016a), A model-based climatology analysis of wind power resources at 100-m height over the Bohai Sea and the Yellow Sea, *Appl. Energy*, *179*, 575–589, doi:10.1002/2015jd024177.
Li, D., H. von Storch, and B. Geyer (2016b), High-resolution wind hindcast over the Bohai Sea and the Yellow Sea in East Asia: Evaluation and wind climatology analysis, *J. Geophys. Res. Atmos.*, *121*, 111–129, doi:10.1002/2015jd024177.
Li, L. L. (2010), Study on the current status and future development of coastal ocean observation system based on observational stations and buoys, Master thesis, 89 pp., Ocean Univ. of China, China.
Liu, P., A. P. Tsimpidi, Y. Hu, et al. (2012), Differences between downscaling with spectral and grid nudging using WRF, *Atmos. Chem. Phys.*, *12*, 3601–3610, doi:10.5194/acp-12-3601-2012.
Lo, J. C.-F., Z.-L. Yang, and R. A. Pielke (2008), Assessment of three dynamical climate downscaling methods using the Weather Research and Forecasting (WRF) model, *J. Geophys. Res.*, *113*, D09112, doi:10.1029/2007JD009216.
Lucas-Picher, P., M. Wulff-Nielsen, J. H. Christensen, G. Aðalgeirsdóttir, R. Mottram, and S. B. Simonsen (2012), Very high resolution regional climate model simulations over Greenland: Identifying added value, *J. Geophys. Res.*, *117*, D02108, doi:10.1029/2011JD016267.
Mahoney, K., M. A. Alexander, G. Thompson, J. J. Barsugli, and J. D. Scott (2012), Changes in hail and flood risk in high-resolution simulations over Colorado's mountains, *Nat. Clim. Change*, *2*, 125–131, doi:10.1038/nclimate1344.
Mesinger, F., et al. (2006), North American Regional Reanalysis, *Bull. Am. Meteorol. Soc.*, *87*, 343–360, doi:10.1175/BAMS-87-3-343.
Miguez-Macho, G., G. L. Stenchikov, and A. Robock (2004), Spectral nudging to eliminate the effects of domain position and geometry in regional climate model simulations, *J. Geophys. Res.*, *109*, D13104, doi:10.1029/2003JD004495.
Onogi, K., et al. (2007), The JRA-25 reanalysis, *J. Meteorol. Soc. Jpn.*, *85*, 369–432.
Parker, R. J., B. J. Reich, and S. R. Sain (2015), A multiresolution approach to estimating the value added by regional climate models, *J. Clim.*, *28*(22), 8873–8887, doi:10.1175/JCLI-D-14-00557.1.
Poli, P., et al. (2016), ERA-20C: An atmospheric reanalysis of the twentieth century, *J. Clim.*, *29*, 4083–4097, doi:10.1175/JCLI-D-15-0556.1.
Prein, A. F., A. Gobiet, M. Suklitsch, H. Truhetz, N. K. Awan, K. Keuler, and G. Georgievski (2013), Added value of convection permitting seasonal simulations, *Clim. Dyn.*, *41*, 26,555–22,677, doi:10.1007/s00382-013-1744-6.
Pryor, S. C., R. J. Barthelmie, D. T. Young, E. S. Takle, R. W. Arritt, D. Flory, W. J. Gutowski, A. Nunes, and J. Roads (2009), Wind speed trends over the contiguous United States, *J. Geophys. Res.*, *114*, D14105, doi:10.1029/2008JD011416.
Prein, A. F., et al. (2015), A review on regional convection-permitting climate modeling: Demonstrations, prospects, and challenges, *Rev. Geophys.*, *53*(2), pp. 323–361, doi:10.1002/2014RG000475.
Pulliainen, J. (2006), Mapping of snow water equivalent and snow depth in boreal and sub-arctic zones by assimilating space-borne microwave radiometer data and ground-based observations, *Remote Sens. Environ.*, *101*, 257–269.
Ramzan, M., S. Ham, M. Amjad, E.-C. Chang, and K. Yoshimura (2017), Sensitivity evaluation of spectral nudging schemes in historical dynamical downscaling for South Asia, *Adv. Meteorol.*, 7560818, doi:10.1155/2017/7560818.
Rockel, B., A. Will, and A. Hense (2008a), The regional climate model COSMO-CLM (CCLM), *Meteorol. Z.*, *17*(4), 347–348.
Rockel, B., et al. (2008b), Dynamical downscaling: Assessment of model system dependent retained and added variability for two different regional climate models, *J. Geophys. Res.*, *113*, D21107, doi:10.1029/2007JD009461.
Rummukainen, M. (2015), Added value in regional climate modeling, *Wiley Interdiscip. Rev. Clim. Change*, *7*, 145–159, doi:10.1002/wcc.378.
Sasaki, H., J. Kida, T. Koide, and M. Chiba (1995), The performance of long term integrations of a limited area model with the spectral boundary coupling method, *J. Meteorol. Soc. Jpn.*, *73*, 165–181.
Schaaf, B., H. von Storch, and F. Feser (2017), Has spectral nudging an effect for dynamical downscaling applied in small (500 km and less) regional climate model domains?, *Mon. Weather Rev.*, doi:10.1175/MWR-D-17-0087.1.
Schubert-Frisius, M., F. Feser, H. von Storch, and S. Rast (2017), Optimal spectral nudging for global dynamic downscaling, *Mon. Weather Rev.*, *145*, 909–927, doi:10.1175/MWR-D-16-0036.1.
Serreze, M. C., M. P. Clark, and D. H. Bromwich (2003), Monitoring precipitation over the Arctic terrestrial drainage system: Data requirements, shortcomings, and applications of atmospheric reanalysis, *J. Hydrometeorol.*, *4*, 387–407.
Small, R. J., E. Curchitser, K. Hedstrom, B. Kauffman, and W. G. Large (2015), The Benguela upwelling system: Quantifying the sensitivity to resolution and coastal wind representation in a global climate model, *J. Clim.*, *28*, 9409–9432, doi:10.1175/JCLI-D-15-0192.1.
Sotillo, M. G., A. W. Ratsimandresey, J. C. Carretero, A. Bentamy, F. Valero, and F. González-Rouco (2005), A high-resolution 44-year atmospheric hindcast for the Mediterranean Basin: Contribution to the regional improvement of global reanalysis, *Clim. Dyn.*, *25*, 219–236, doi:10.1007/s00382-005-0030-7.
Stevens, B., et al. (2013), Atmospheric component of the MPI-M earth system model: ECHAM6: ECHAM6, *J. Adv. Model. Earth Syst.*, *5*, 146–172, doi:10.1002/jame.20015.
Sterl, A. (2004), On the (in) homogeneity of reanalysis products, *J. Clim.*, *17*(19), 3866–3873.
Takala, M., K. Luojus, J. Pulliainen, C. Derksen, J. Lemmetyinen, J.-P. Kärnä, J. Koskinen, and B. Bojkov (2011), Estimating northern hemisphere snow water equivalent for climate research through assimilation of space-borne radiometer data and ground-based measurements, *Remote Sens. Environ.*, *115*, 3517–3529, doi:10.1016/j.rse.2011.08.014.
Takala, M., J. Pulliainen, S. Metsamaki, and J. Koskinen (2009), Detection of snowmelt using spaceborne microwave radiometer data in Eurasia from 1979 to 2007, *IEEE Geosci. Remote Sens. Lett.*, *47*, 2996–3007, doi:10.1109/TGRS.2009.2018442.
Tim, N., E. Zorita, and B. Hünicke (2015), Decadal variability and trends of the Benguela upwelling system as simulated in a high-resolution ocean simulation, *Ocean Sci.*, *11*, 483–502, doi:10.5194/os-11-483-2015.
Torma, C., F. Giorgi, and E. Coppola (2015), Added value of regional climate modeling over areas characterized by complex terrain-precipitation over the Alps, *J. Geophys. Res. Atmos.*, *120*, 3957–3972, doi:10.1002/2014jd022781.
Uppala, S. M., et al. (2005), The ERA-40 re-analysis, *Q. J. R. Meteorol. Soc.*, *131*, 2961–3012, doi:10.1256/qj.04.176.
von Storch, H. (1978), Construction of optimal numerical filters fitted for noise damping in numerical simulation models, *Beitr. Phys. Atmos.*, *51*, 189–197.
von Storch, H., H. Langenberg, and F. Feser (2000), A spectral nudging technique for dynamical downscaling purposes, *Mon. Weather Rev.*, *128*, 3664–3673, doi:10.1175/1520-0493(2000)128<3664:ASNTFD>2.0.CO;2.
Waldron, K. M., J. Paegle, and J. D. Horel (1996), Sensitivity of a spectrally filtered and nudged limited-area model to outer model options, *Mon. Weather Rev.*, *124*, 529–547, doi:10.1175/1520-0493(1996)124<0529:SOASFA>2.0.CO;2.
Wang, J., and V. R. Kotamarthi (2013), Assessment of dynamical downscaling in near-surface fields with different spectral nudging approaches using the Nested Regional Climate Model (NRCM), *J. Appl. Meteorol. Climatol.*, *52*, 1576–1591, doi:10.1175/jamc-d-12-0302.1.
Weisse, R., et al. (2015), Climate services for marine applications in Europe, *Earth Perspect.*, *2–3*, doi:10.1186/s40322-015-0029-0.
Weisse, R., H. Heyen, and H. von Storch (2000), Sensitivity of a regional atmospheric model to a sea state dependent roughness and the need of ensemble calculations, *Mon. Weather Rev.*, *128*, 3631–3642.

Weisse, R., et al. (2009), Regional meteorological–marine Reanalyses and climate change projections: Results for Northern Europe and potential for coastal and offshore applications, *Bull. Am. Meteorol. Soc.*, *90*, 849–860, doi:10.1175/2008BAMS2713.1.

Weisse, R., L. Gaslikova, B. Geyer, N. Groll, and E. Meyer (2014), coastDat—Model data for science and industry, *Die Küste*, *81*, 5–18.

Weisse, R., and F. Feser (2003), Evaluation of a method to reduce uncertainty in wind hindcasts performed with regional atmosphere models, *Coastal Eng.*, *48*(4), 211–225.

Winterfeldt, J., and R. Weisse (2009), Assessment of value added for surface marine wind speed obtained from two regional climate models, *Mon. Weather Rev.*, *137*, 2955–2965.

Winterfeldt, J., B. Geyer, and R. Weisse (2011), Using QuikSCAT in the added value assessment of dynamically downscaled wind speed, *Int. J. Climatol.*, *31*, 1028–1039.

Wu, W., A. H. Lynch, and A. Rivers (2005), Estimating the uncertainty in a regional climate model related to initial and lateral boundary conditions, *J. Clim.*, *18*, 917–933, doi:10.1175/JCLI-3293.1.

Yang, S., K.-M. Lau, and K.-M. Kim (2002), Variations of the east Asian jet stream and Asian–Pacific–American winter climate anomalies, *J. Clim.*, *15*, 306–325, doi:10.1175/1520-0442(2002)015<0306:VOTEAJ>2.0.CO;2.

Yoshimura, K., and M. Kanamitsu (2008), Dynamical global downscaling of global reanalysis, *Mon. Weather Rev.*, *136*, 2983–2998, doi:10.1175/2008MWR2281.1.

Zahn, M., H. von Storch, and S. Bakan (2008), Climate mode simulation of North Atlantic polar lows in a limited area model, *Tellus A*, *60*, 620–631, doi:10.1111/j.1600-0870.2008.00330.x.